# Exploring the anti-glioma mechanism of the active components of Cortex Periplocae based on network pharmacology and iTRAQ proteomics in vitro

Jing Huan<sup>1,2,A–F</sup>, Cui-Ping You<sup>3,A–F</sup>, Yu-Cheng Lu<sup>3,4,A–F</sup>, Feng-Yuan Che<sup>1,5,A,F</sup>

- <sup>1</sup> Institute of Clinical Medicine College, Guangzhou University of Chinese Medicine, China
- <sup>2</sup> Department of Acupuncture and Moxibustion, Linyi People's Hospital, China
- <sup>3</sup> Central Laboratory, Linyi People's Hospital, China
- <sup>4</sup> Biobank, Linyi People's Hospital, China
- <sup>5</sup> Department of Neurology, Linyi People's Hospital, China
- A research concept and design; B collection and/or assembly of data; C data analysis and interpretation;
- D writing the article; E critical revision of the article; F final approval of the article

Advances in Clinical and Experimental Medicine, ISSN 1899-5276 (print), ISSN 2451-2680 (online)

Adv Clin Exp Med. 2023;32(11):1279-1290

### Address for correspondence

Feng-Yuan Che E-mail: chefy2020@163.com

### **Funding sources**

None declared

#### **Conflict of interest**

None declared

Received on May 23, 2022 Reviewed on September 14, 2022 Accepted on February 27, 2023

Published online on October 30, 2023

#### Cite as

Huan J, You CP, Lu YC, Che FY. Exploring the anti-glioma mechanism of the active components of Cortex Periplocae based on network pharmacology and iTRAQ proteomics in vitro. *Adv Clin Exp Med*. 2023;32(11):1279–1290. doi:10.17219/acem/161724

#### DOI

10.17219/acem/161724

### Copyright

Copyright by Author(s)
This is an article distributed under the terms of the
Creative Commons Attribution 3.0 Unported (CC BY 3.0)
(https://creativecommons.org/licenses/by/3.0/)

### **Abstract**

**Background.** The active components of Cortex Periplocae (CP) exert antitumor properties in many cancers. However, little is known about their effects on glioma or the related underlying mechanisms.

**Objectives.** The study investigated the underlying mechanism of CP in treating glioma.

**Materials and methods.** The U251 and TG905 cells were treated with an ethanol extract from CP. Cell proliferation was detected using Cell Counting Kit-8 (CCK-8) and a colony formation assay. The flow cytometric analysis was applied to explore the induction of cell cycle arrest and apoptosis. The expression levels of cell cycle- and apoptosis-associated proteins were measured with western blot. A network pharmacology method was performed to predict the potential mechanism underlying the effects of the active components of CP on glioma. Then, isobaric tags for relative and absolute quantitation (iTRAQ)-based quantitative proteomics analysis was used to verify the differentially expressed proteins and pathways in order to reveal the underlying mechanisms. Furthermore, to determine the iTRAQ results, 6 candidate proteins were chosen for quantification using parallel reaction monitoring (PRM).

**Results.** The CP extract inhibited the proliferation of U251 and TG905 cells and induced cell cycle arrest and apoptosis. There are 16 active compounds of CP. The antitumor mechanism of CP may be related to the apoptosis pathway, p53 signaling pathway, P13K-AKT pathway, or transcriptional misregulation in cancer pathway. Six proteins (HSP90AB1, T0P2A, ATP1A1, TGFβ1, ATP1B1, and TYMS) were determined to be key factors involved in regulating CP in glioma.

**Conclusions.** Our research revealed the underlying mechanism of CP in treating glioma using integrated network pharmacology and iTRAQ-based quantitative proteomics technology.

Key words: proteomics, glioma, network pharmacology, Cortex Periplocae

# Introduction

Gliomas, a group of life-threatening tumors, are the most common primary intracranial tumors. They arise from precursor or glial cells of the central nervous system,2 and the mortality rate remains high despite advancements in currently available therapeutic approaches, including surgical treatment, radiotherapy and chemotherapy.<sup>3</sup> It is difficult to resect the tumor completely due to its infiltrative growth and critical localization in the brain.4 The 5-year survival rate of patients with malignant glioma was reported to be less than 25% when treated by surgery alone. Gliomas are not sensitive to radiotherapy, and the blood-brain barrier makes it difficult for chemotherapeutic drugs to penetrate. Furthermore, radiotherapy and chemotherapy cause complications8 that negatively impact the quality of life of patients. Thus, there is an urgent need to find more satisfactory treatment methods for glioma.

Cortex Periplocae (CP), called Xiangjiapi in Chinese, is the dry root of the Chinese herb *Periploca sepium* Bunge, a Traditional Chinese Medicine (TCM) medicament. It has a long history of use in the treatment of autoimmune diseases, such as rheumatoid arthritis.9 Recently, additional research has explored the biological activity of the crude extract and the active components of CP, such as anticancer, 10 cardiotonic 11 and anti-inflammatory effects, 12,13 to determine its potential pharmaceutical value. Li et al. found that the periplocin isolated from CP significantly inhibited the proliferation of gastric cancer cells and induced apoptosis in vivo and in vitro by the ERK1/2-EGR1 pathway.14 Moreover, periplocin inhibited the growth of pancreatic cancer by inducing apoptosis through AMPKmTOR signaling.<sup>10</sup> As a potential antitumor component, periplocin has also been reported to inhibit the growth of colon cancer<sup>15</sup> and lung cancer<sup>16</sup> through β-catenin/ TCF signaling and the AKT/ERK signaling pathway, respectively. Yang et al. suggested that periplogenin (PPG) isolated from CP triggers the apoptosis of colon cancer cells through the IRE<sub>1α</sub>-ASK1-JNK and BIP-eIF<sub>2α</sub>-CHOP signaling pathways.<sup>17</sup> The PPG also has a clear effect on the treatment of nasopharyngeal carcinoma.<sup>18</sup> Moreover, lupeol acetate from CP showed an inhibitory effect in esophageal tumorigenesis in rats. 19 However, the effects of CP extract and its underlying mechanisms in treating glioma remain to be determined.

Due to the rapid advancements in bioinformatics, network pharmacology and isobaric tags for relative and absolute quantitation (iTRAQ) proteomics approaches have been effectively used to reveal the active components of TCM medicaments and their potential mechanisms of action. <sup>20</sup> A new methodological strategy, network pharmacology, provides a significant advantage in helping to understand the therapeutic mechanism of TCM medicaments. <sup>21</sup> The CP has antitumor activities exerted through a multi-component, multi-target, multi-pathway, and multi-biological process, which conforms to the features of network pharmacology. <sup>22</sup>

The iTRAQ approach has been employed to quantify and qualify proteins, as well as explore potential protein interactions. <sup>23,24</sup> In this study, network pharmacology and iTRAQ proteomics were applied to explore the active components of CP and its anti-glioma molecular mechanisms.

# **Objectives**

The purpose of this study is to investigate the underlying mechanisms of CP in treating glioma.

# **Materials and methods**

# Preparation of the ethanol extract of Cortex Periplocae

The CP was obtained from Linyi People's Hospital (Linyi, China). First, 100 g of CP was crushed and mixed with 75% ethanol in a ratio of 1:10, then placed in the dark overnight. The mixture was sonicated for 30 min, removing the filtrate, and the process was repeated 3 times. The filtered solution was centrifuged at 10,000 rpm for 8 min to obtain the supernatant, using a Buchi rotary evaporator (Buqi, Gent, Belgium). The ethanol extract was freeze-dried and separated, and 92.18 g of freeze-dried powder was obtained from the extract. A total of 100 mg of ethanol extract of CP was added to 1 mL dimethyl sulfoxide (DMSO) to prepare a stock solution with a concentration of 100 mg/mL.

### Cell lines and cell culture

The U251 and TG905 were obtained from the Cellular Biology Institute of the Shanghai Academy of Sciences (Shanghai, China). All cells were cultured in RPMI-1640, adding 10% fetal bovine serum (FBS) at 37°C in a 5%  $\rm CO_2$  atmosphere.

### **CCK-8** assay

The cells were treated with CP (0  $\mu$ g/mL, 1  $\mu$ g/mL, 3  $\mu$ g/mL, 10  $\mu$ g/mL, 30  $\mu$ g/mL, and 100  $\mu$ g/mL) for the corresponding time (24 h, 48 h and 72 h). Then, the cells were added to a mixture of Cell Counting Kit-8 (CCK-8) (BB-4202; Dojindo Laboratories, Kumamoto, Japan) and Dulbecco's modified Eagle medium (DMEM), and incubated for another hour. The absorbance at a wavelength of 450 nm was recorded using a microplate reader (BestBio, Shanghai, China).

### **Colony formation assay**

A total of 200 cells were planted in each hole of a 6-well plate. After 24 h, different concentrations of CP were added to the cells for approx. 10 days. The colonies were fixed

with 4% paraformaldehyde and stained with 0.1% crystal violet. The images were captured with a digital camera (Fluorchem E; Proteinsimple, Santa Clara, USA).

# Flow cytometric analysis

The cells were harvested and fixed with 75% ethanol overnight. After washing and resuspension in phosphate-buffered saline (PBS), the cells were stained with propidium iodide (PI)/RNase staining buffer for 15 min. Finally, the samples were used for the analysis in a flow cytometer (LSRFortessa<sup>TM</sup> SORP; BD Biosciences, Franklin Lakes, USA).

### **Apoptosis assay**

An FITC Annexin V Apoptosis Detection Kit (BB-4101) (BD Biosciences) was used to measure the apoptosis rate. The cells were harvested, washed and resuspended in IX binding buffer. Five microliters of PI and Annexin X were added to the solution, respectively, and incubated in the dark for 5 min. Finally, the samples were used for analysis in a flow cytometer.

### Western blot

After treatments, cells were lysed using radioimmunoprecipitation assay (RIPA) with phosphatase inhibitor. The cellular protein was extracted and quantified with the bicinchoninic acid (BCA) method. Similar amounts of protein were loaded and separated using sodium dodecylsulfate polyacrylamide gel electrophoresis (SDS-PAGE), and transferred to polyvinylidene fluoride (PVDF) membranes. The membranes were exposed to specific primary antibodies and fluorescent secondary antibodies after being blocked in a 5% non-fat dry milk solution. The primary antibodies were monoclonal mouse antibodies against cyclin E, CDK2 (Cell Signaling Technology, Danvers, USA), poly (ADP-ribose) polymerase (PARP), cleaved caspase-3, caspase-3 (Abcam, Cambridge, UK), and GAPDH (Santa Cruz Biotechnology, Dallas, USA). The chemiluminescent detection was used to visualize the membrane samples (MilliporeSigma, Burlington, USA). The respective densities of the protein bands were evaluated using ImageJ software (National Institutes of Health, Bethesda, USA).

# **Identification of candidate compounds**

All of the CP compounds were retrieved from the TCM Systems Pharmacology Database and Analysis Platform (TCMSP), which includes 500 Chinese herbal medicines with 30,069 ingredients through database integration and literature mining. The pharmacokinetic properties of natural compounds involve oral bioavailability (OB), drug-likeness (DL) and Caco-2 cells, which were provided for study.

# Screening of active compounds

Among the ADME (absorption, distribution, metabolism, and excretion) properties of the compounds, OB, DL and Caco-2 cells represent the most vital properties of the administered drugs. Oral bioavailability is used to assess the efficiency of the drug distribution within systemic circulation. Drug-likeness refers to a measure of similarities between the compound and known drugs. The average DL index of all of the drugs was  $0.18.^{25}$  The Caco-2 cells can be used to investigate intestinal epithelium permeability. Based on the TCMSP database, molecules with Caco-2 > -0.40 corresponded to good permeability in the small intestinal epithelium. Hence, in this study, molecules with OB  $\geq$  30%, DL  $\geq$  0.18 and Caco-2 > -0.40 were considered active compounds.

# Target identification through integrated database analyses

The TCMSP database was used to identify the active components of CP, while GeneCards database (https://genecards.weizmann.ac.il/v3/) was used to discover gliomaspecific therapeutic targets. The overlap between the 2 results provided drug targets for CP in treating glioma.

# Protein extraction, enzymatic hydrolysis and peptide quantification

Total protein was extracted from U251 cells with SDT (4% (w/v) SDS, 100 mM Tris/HCl 1 mM dithiothreitol (DTT), pH 7.6). The extracted proteins were quantified using a BCA kit. Protein enzymatic hydrolysis was performed using the filter-aided sample preparation (FASP) procedure. The enzymolysis peptide was desalted with the use of a C18 purification cartridge, freeze-dried and re-dissolved with 40  $\mu$ L of the dissolution buffer. Finally, the peptides were quantified with OD280.

### iTRAQ and LC-MS/MS

Equal amounts of each peptide were taken and labeled according to the AB SCIEX iTRAQ labeling kit instructions. <sup>30</sup> Samples were labeled as iTRAQ-113, -114, -115, and -116, -117, -118. The labeled peptides were mixed in equal amounts and graded with an AKTA Purifier 100 (GE Healthcare, Chicago, USA). Liquid chromatography—mass spectrometry (LC—MS)/MS was carried out as described by Ross et al. <sup>30</sup>

# Mass spectrometry data processing and analysis

The original raw data obtained using LC–MS/MS were identified and quantified with mascot and proteome discoverer. Table of SI is shown in the main library parameters.

# **Bioinformatic analysis**

The Gene Ontology (GO) analysis was performed using the Blast2 GO database (http://geneontology.org/). The KEGG Automatic Annotation Server (KASS) software (https://www.genome.jp/kegg/kaas/) was used to classify and group the identified proteins. The distribution of Kyoto Encyclopedia of Genes and Genomes (KEGG; http://www.genome.jp/kegg/) pathways and whole protein sets for each GO classification were compared using Fisher's exact test. The GO annotation or KEGG pathway annotation was used to enrich the target protein set.

The complex Heatmap R package (R Foundation for Statistical Computing, Vienna, Austria) was employed to categorize the expression of proteins and samples at the same time, as well as to create a hierarchical clustering heatmap.

The information obtained from the IntAct or STRING database was used to find direct and indirect interaction relationships between the target proteins. The interaction network was generated and analyzed using Cytoscape (https://cytoscape.org/).

# Parallel reaction monitoring verification

Protein extraction was carried out as described above for the iTRAQ experiment. Then, the samples were added to DTT, boiled in a water bath for 15 min, cooled down, and UA (8 M urea, 150 mM Tris-HCl, pH 8.0) buffer was added. The samples were then transferred to a 10 kd ultrafiltration tube and centrifuged at  $14,000 \times g$  for 30 min. A total of 200 µL of UA buffer was added, then the samples were centrifuged and the filtrate was discarded. Next, indole-3-acetic acid (IAA) was added, the sample was shaken and centrifuged at  $14,000 \times g$  for 20 min. Then, the NH<sub>4</sub>HCO<sub>3</sub> buffer (50 mM) was added, and the sample was centrifuged at 14,000 g for 20 min twice. A new collecting pipe was used and the sample was centrifuged for 15 min. A total of 40 μL of NH<sub>4</sub>HCO<sub>3</sub> buffer (50 mM) was added, the sample was centrifuged again for 30 min, and the filtrate was collected. After enzymatic hydrolysis, the collected peptide was desalted and lyophilized, then re-dissolved with 0.1% formic acid (FA). The peptide concentration was established using OD280.

According to the pre-experimental results, 10 target peptides of 6 identified target proteins were quantified using parallel reaction monitoring (PRM). In order to set up the PRM method, peptide information was entered into Xcalibur software (Thermo Fisher Scientific, Waltham, USA). The standard peptide was mixed with about 1  $\mu$ g of peptide extracted from each sample for detection. High-performance liquid chromatography (HPLC) was used for chromatographic separation. The chromatographic column reached liquid equilibrium at 95% A.

The samples separated with HPLC were analyzed using PRM mass spectrometry (Q Exactive HF mass spectrometer; Thermo Fisher Scientific, Waltham, USA).

The PRM was detected in 6 samples, and finally, the data from the original PRM files were analyzed using Skyline software (Skyline Software Systems, Inc., Herndon, USA).

# Statistical analysis

In this study, GraphPad Prism v. 8.2.1 (GraphPad Software, San Diego, USA) was used for data analysis. Data were expressed as mean  $\pm$  standard deviation (M  $\pm$ SD) and were obtained from at least 3 separate experiments. The significance levels of differences were determined with independent sample t-tests for the various treatments. A value of p < 0.05 was considered statistically significant.

### Results

### CP inhibits cell viability of glioma cells

The CP with different concentrations (0  $\mu$ g/mL, 1  $\mu$ g/mL, 3  $\mu$ g/mL, 10  $\mu$ g/mL, 30  $\mu$ g/mL, and 100  $\mu$ g/mL) were added to the U251 and TG905 cells for 24 h, 48 h and 72 h, and cell viability was measured with a CCK-8 assay. As shown in Fig. 1A,B, CP suppressed cell viability in a time- and dose-dependent manner. For U251 cells, the IC50 values of CP at 24 h, 48 h and 72 h were 26.48  $\mu$ g/mL, 11.07  $\mu$ g/mL and 3.349  $\mu$ g/mL, respectively. For TG905 cells, the IC50 values of CP at each of the 3 time intervals were 30.39  $\mu$ g/mL, 11.1  $\mu$ g/mL and 12.7  $\mu$ g/mL, respectively. Furthermore, a colony formation assay showed that CP degraded the rate of colony formation in U251 and TG905 cells in a dose-dependent manner (Fig. 1C).

# CP induces cell cycle arrest in glioma cells

Flow cytometry results showed that CP caused a large accumulation of glioma cells in G0/G1 phases in a dose-dependent manner, which was accompanied by a decrease in S and G2/M phases (Fig. 2A). In addition, western blotting was used to explore the expression level of cyclin E and CDK2, 2 cell cycle-associated proteins (Fig. 2C). The results showed that a high concentration (16  $\mu$ g/mL and 32  $\mu$ g/mL) of CP downregulated the expression level of cyclin E and CDK2, but a low concentration (8  $\mu$ g/mL) of CP had no effect on the protein expression (Fig. 2B). The above results indicate that CP may have inhibited cell proliferation resulting from G0/G1 cell cycle arrest.

# Treatment of glioma cells with CP induces apoptosis

To investigate whether CP induced apoptosis in glioma cells, CP (0  $\mu$ g/mL, 8  $\mu$ g/mL, 16  $\mu$ g/mL, and 32  $\mu$ g/mL)

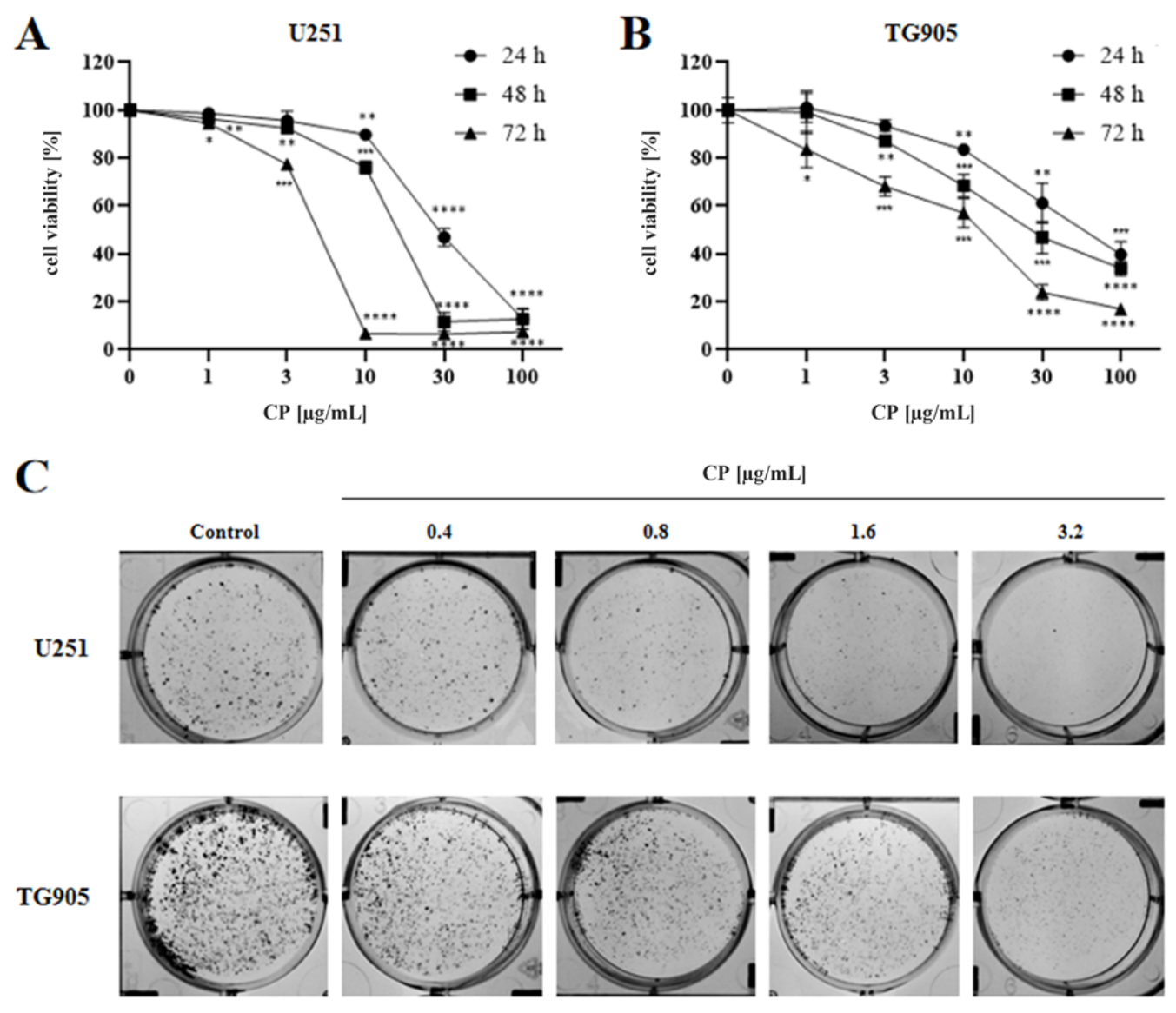


**Fig. 1.** Cortex Periplocae (CP) inhibits cell viability of glioma cells. A,B. U251 and TG905 cells were treated with CP (0  $\mu$ g/mL, 1  $\mu$ g/mL, 3  $\mu$ g/mL, 30  $\mu$ g/mL, and 100  $\mu$ g/mL) for 24 h, 48 h and 72 h. Cell viability was measured using Cell Counting Kit-8 (CCK-8) assay (n = 3); C. U251 and TG905 cells were treated with CP (0  $\mu$ g/mL, 0.4  $\mu$ g/mL, 0.8  $\mu$ g/mL, 1.6  $\mu$ g/mL, and 3.2  $\mu$ g/mL) for approx. 10 days. The rate of colony formation was evaluated with colony formation assay (n = 3)

was added to U251 and TG905 cells for 48 h, and then flow cytometry with Annexin V-FITC staining was used to detect the number of apoptotic cells. The results showed that the treatment of U251 and TG905 cells with CP induced apoptosis. Apoptotic cells in the U251 and TG905 samples after CP treatment ranged from 4.1% to 64.9% (p < 0.0001) and from 4.04% to 86.9% (p < 0.0001), respectively (Fig. 3A,B). To further reveal the potential mechanisms involved in CP-induced apoptosis, western blotting was used to establish the level of apoptosis-related proteins, namely PARP, caspase-3 and cleaved caspase-3. The data showed that CP decreased the expression level of caspase-3 and PARP, while upregulating the level of cleaved caspase-3 in a dose-dependent manner (Fig. 3C).

### Identification of the active compounds of CP

To identify the active compounds of CP, the TCMSP database was used, and 79 components of CP were found. Among the 79 compounds in CP, 16 satisfied the criterion of OB  $\geq$  30%, DL  $\geq$  0.18 and Caco-2 > -0.40. Detailed information for the 16 compounds is shown in Table 1. The data demonstrated that CP was chemically fit for drug development.

### Drug targets of CP for treating glioma

The TCMSP database was further used to predict the putative targets of CP. Nineteen putative targets of CP remained after removing duplicates. Meanwhile, 5753 validated therapeutic targets for glioma and glioblastoma

<sup>\*</sup> p < 0.05; \*\* p < 0.01; \*\*\* p < 0.001; \*\*\*\* p < 0.0001 compared to the control group.

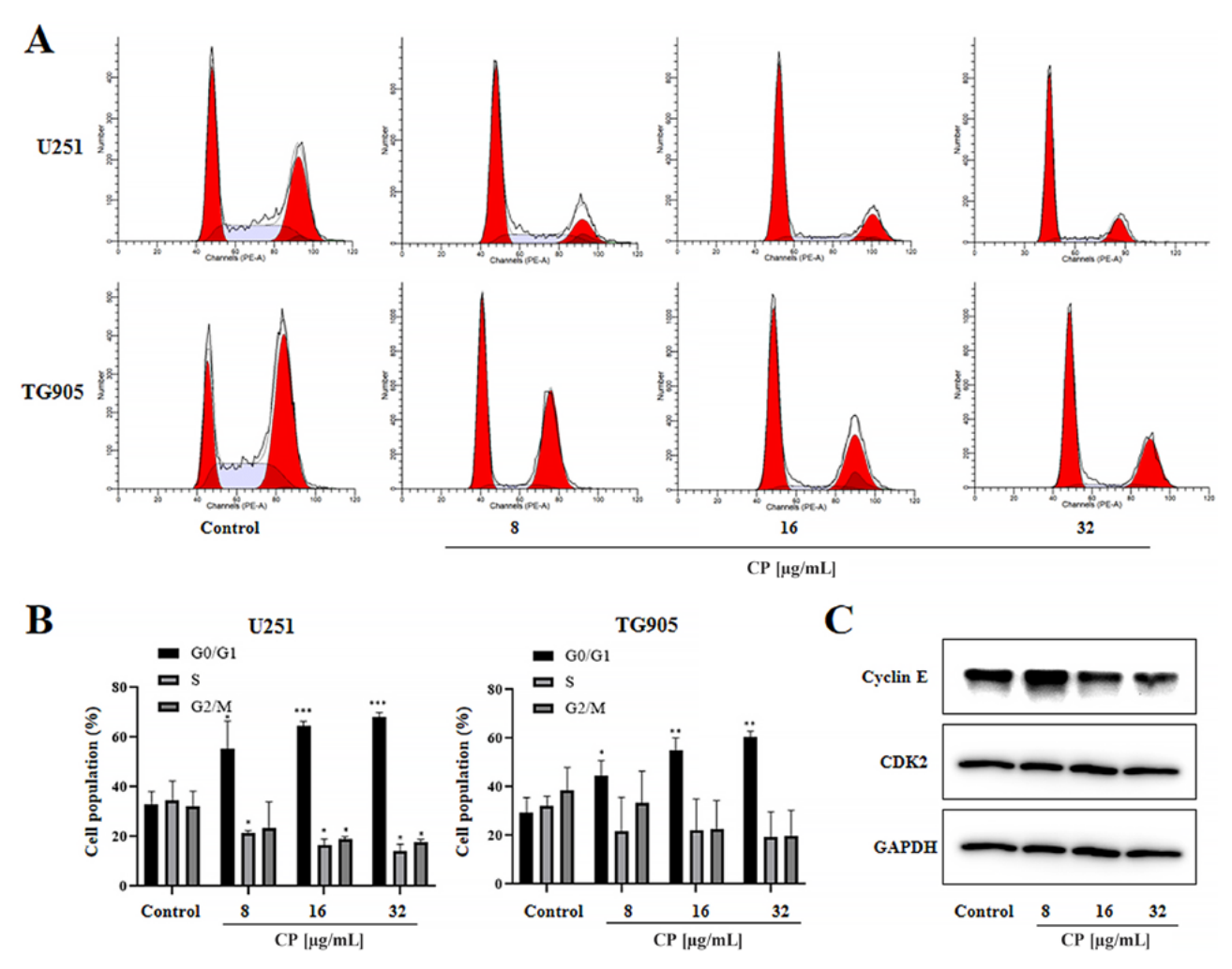


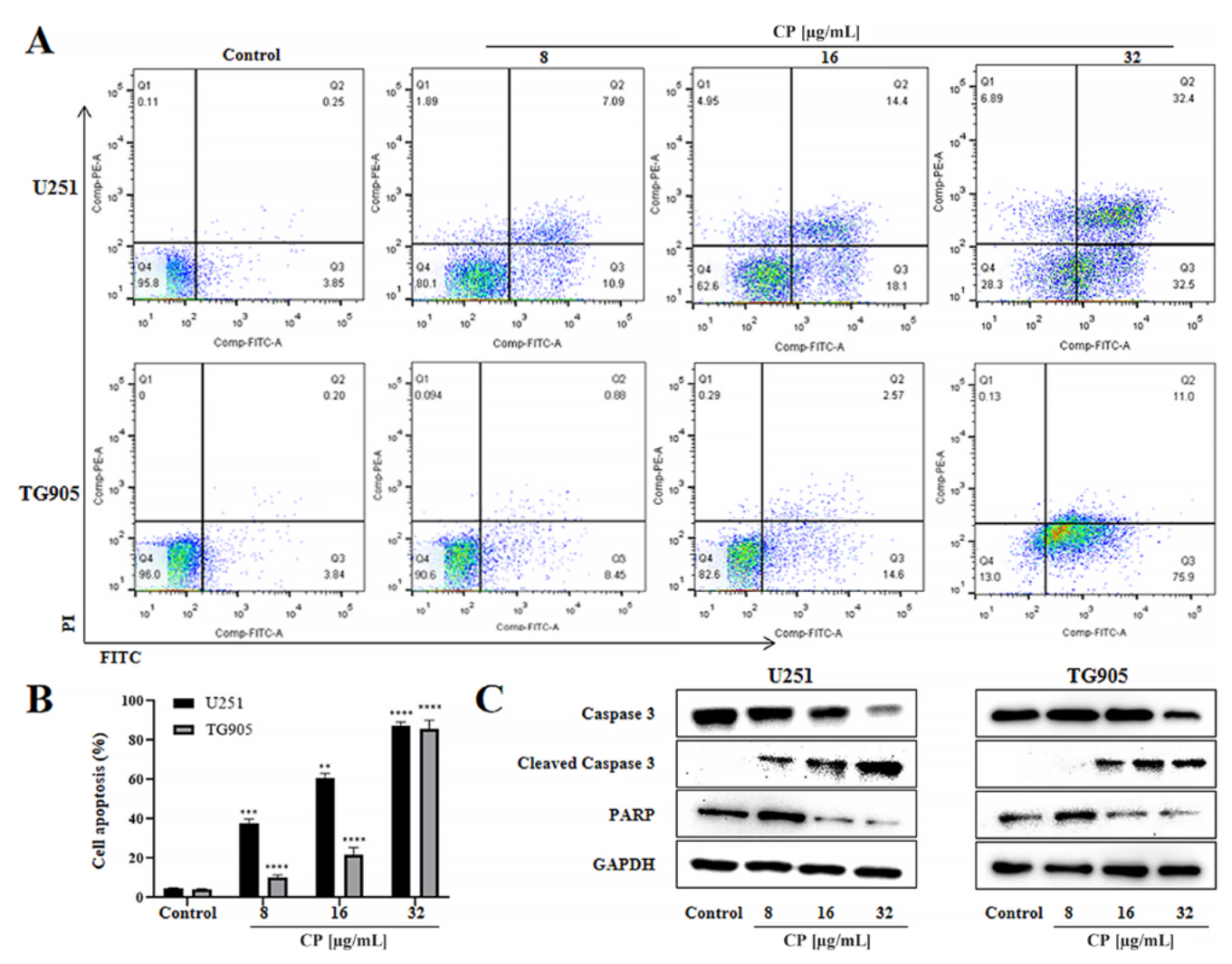
Fig. 2. Cortex Periplocae (CP) induces cell cycle arrest in glioma cells. The U251 and TG905 cells were treated with CP (0  $\mu$ g/mL, 8  $\mu$ g/mL, 16  $\mu$ g/mL, and 32  $\mu$ g/mL) for 24 h. A,B. The cell cycle distribution was analyzed with flow cytometry (n = 3); C. The expression level of cyclin E and CDK2 was detected with western blot

Table 1. The active components of Cortex Periplocae (CP)

Mol ID	Molecule name	OB [%]	DL	Caco-2
MOL001771	poriferast-5-en-3beta-ol	36.91	0.75	1.45
MOL000358	beta-sitosterol	36.91	0.75	1.32
MOL000359	sitosterol	36.91	0.75	1.32
MOL005645	21-O-Methyl-5,14-pregndiene-3β,14β,17β,21-tetrol-20-one	38.52	0.57	0.08
MOL005646	21-O-Methyl-5-pregnene-3β,14β,17β,20,21-pentol	45.12	0.6	-0.04
MOL005652	glycoside K_qt	31.91	0.43	0.79
MOL005654	glycoside H2_qt	49.95	0.48	0.11
MOL005656	glycozolidal	78.07	0.2	1
MOL005658	periplogenin	36.61	0.74	0.04
MOL005664	glycoside E_qt	40.57	0.47	0.39
MOL005666	periplocoside M_qt	32	0.88	0.06
MOL005683	delta 5-pregnenetriol	35.94	0.47	0.17
MOL005686	periplocoside O_qt	32	0.88	0.1
MOL005690	periplocymarin_qt	104.15	0.74	-0.14
MOL005692	neridienone A	30.96	0.48	0.49
MOL005693	xysmalogenin	54.41	0.72	0.02

 ${\sf OB-oral\ bioavailability; DL-drug-likeness.}$ 

<sup>\*</sup> p < 0.05; \*\* p < 0.01; \*\*\* p < 0.001 compared to the control group.



**Fig. 3.** Treatment of glioma cells with Cortex Periplocae (CP) induces apoptosis. The U251 and TG905 cells were treated with CP (0  $\mu$ g/mL, 8  $\mu$ g/mL, 16  $\mu$ g/mL, and 32  $\mu$ g/mL) for 48 h. A,B. Early and late apoptotic cells were analyzed using flow cytometry with Annexin V-FITC staining (n = 3); C. The apoptosis-related proteins, namely cleaved caspase-3, caspase-3 and poly (ADP-ribose) polymerase (PARP) were analyzed using western blot

<sup>\*\*</sup> p < 0.01; \*\*\* p < 0.001; \*\*\*\* p < 0.0001 compared to the control group.

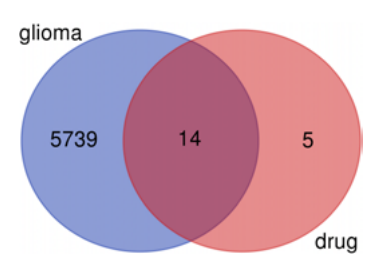


Fig. 4. Drug targets of Cortex Periplocae (CP) for treating glioma. A Venn diagram of constituent-related targets and glioma therapeutic-related targets

were acquired from GeneCards after removing duplicates. The 2 gene target groups were compared, and 14 overlapping genes were ultimately identified (Fig. 4). These 14 target genes were subjected to further analysis (Table 2).

# Quantitative proteomic response to CP

Next, untreated and CP-treated (20  $\mu g/mL$ ) U251 cells were evaluated using iTRAQ/tandem mass tag (TMT) technology to identify peptides, quantify proteins and analyze

Table 2. Target gene of Cortex Periplocae (CP) for treating glioma

Table 2. larget gene or cortex remplocae (er ) for treating gilloma					
Molecule name	Gene symbol	Gene ID			
Apoptosis regulator Bcl-2	BCL2	596			
Muscarinic acetylcholine receptor M1	CHRM1	1128			
Muscarinic acetylcholine receptor M4	CHRM4	1132			
Progesterone receptor	PGR	5241			
Muscarinic acetylcholine receptor M3	CHRM3	1131			
Serum paraoxonase/arylesterase 1	PON1	5444			
Caspase-3	CASP3	836			
Gamma-aminobutyric acid receptor subunit alpha-1	GABRA1	2554			
Caspase-9	CASP9	841			
Caspase-8	CASP8	842			
Glucocorticoid receptor	NR3C1	2908			
Muscarinic acetylcholine receptor M2	CHRM2	1129			
Prostaglandin G/H synthase 1	PTGS1	5742			
Protein kinase C alpha type	PRKCA	5578			

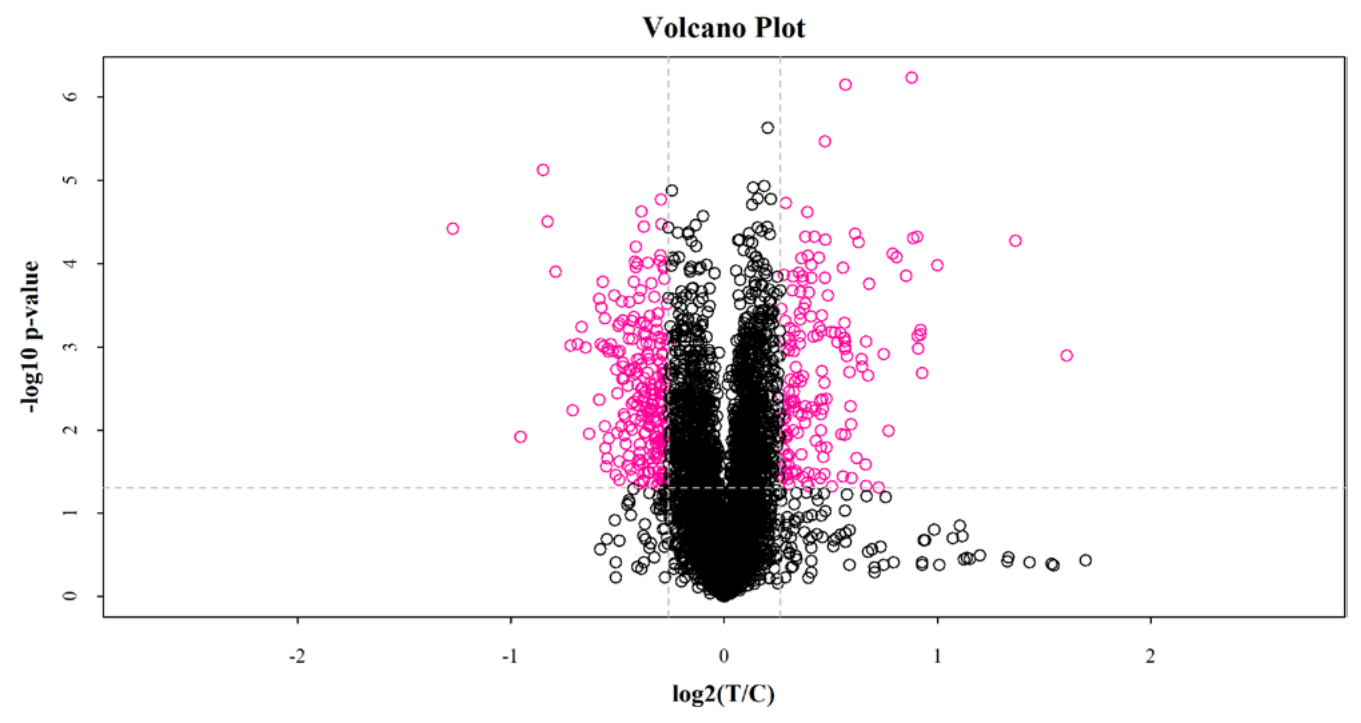


Fig. 5. Volcano plot of differentially expressed proteins in Cortex Periplocae (CP)-treated cells. All proteins were plotted with  $\log_2$  fold change on the x-axis and  $-\log_{10}$  (p-value) on the y-axis. The red dots indicate significantly differentially expressed proteins (up >1.2 or down <0.83). The red dots on the left indicate underexpressed proteins. The red dots on the right indicate overexpressed proteins. The black dots are proteins with no differences in the CP-treated group compared with the control group (n = 3)

Table 3. Statistics on the protein identification results

Datab	ase	Peptides	Unique peptides	Protein groups	Upregulated	Downregulated	Significantly different proteins
Swissport_	Human	40,288	36,930	5482	166	230	369

differentially expressed proteins. As shown in Table 3, 40,288 peptides, including 36,930 unique peptides, were detected, and 5482 proteins were identified. Among the 5482 proteins, a change in expression greater than 1.2-fold (up >1.2 or down <0.83) and a significance level of p < 0.05 were the criteria set for screening the differentially expressed proteins. The National Center for Biotechnology Information (NCBI) Basic Local Alignment Search Tool (BLAST) resource was used to screen differentially expressed proteins. There were 369 differentially expressed proteins, including 166 upregulated and 203 downregulated. The quantitative statistical results are presented using a volcano plot (Fig. 5).

### **Gene Ontology analysis**

In proteomics, the collection of all proteins in a cell, tissue or organism is the major object of study. For high-throughput omics, it is a priority to understand which functions or biological pathways are significantly affected by biological treatments. Thus, proteins and their functions should be analyzed and summarized more systematically. All proteins identified in this project were subjected to GO functional annotation. Then, the GO enrichment

analysis was performed for differentially expressed proteins using Fisher's exact test.

The 369 differentially expressed proteins were categorized into biological process (BP), molecular function (MF) and cellular component (CC), based on their annotation (Fig. 6). The BP analysis revealed that most of the proteins were primarily involved in cellular potassium ion homeostasis, cell proliferation, keratinization, macrophage activation, and intermediate filament bundle assembly. The significant enrichment of CC was mainly related to cytokine activity, receptor regulator activity, receptor-ligand activity, DNA-binding transcription activator activity, RNA polymerase IIspecific and sodium-potassium-exchanging ATPase activity. According to the MF analysis, some proteins were clearly enriched in keratin filament, intermediate filament, sodium-potassium-exchanging ATPase complex, condensed chromosome outer kinetochore, and ATPase-dependent transmembrane transport complex. Additionally, cellular process, biological regulation, regulation of biological process, metabolic process, binding, catalytic activity, cell, cell part, and organelle changed significantly (Fig. 7).

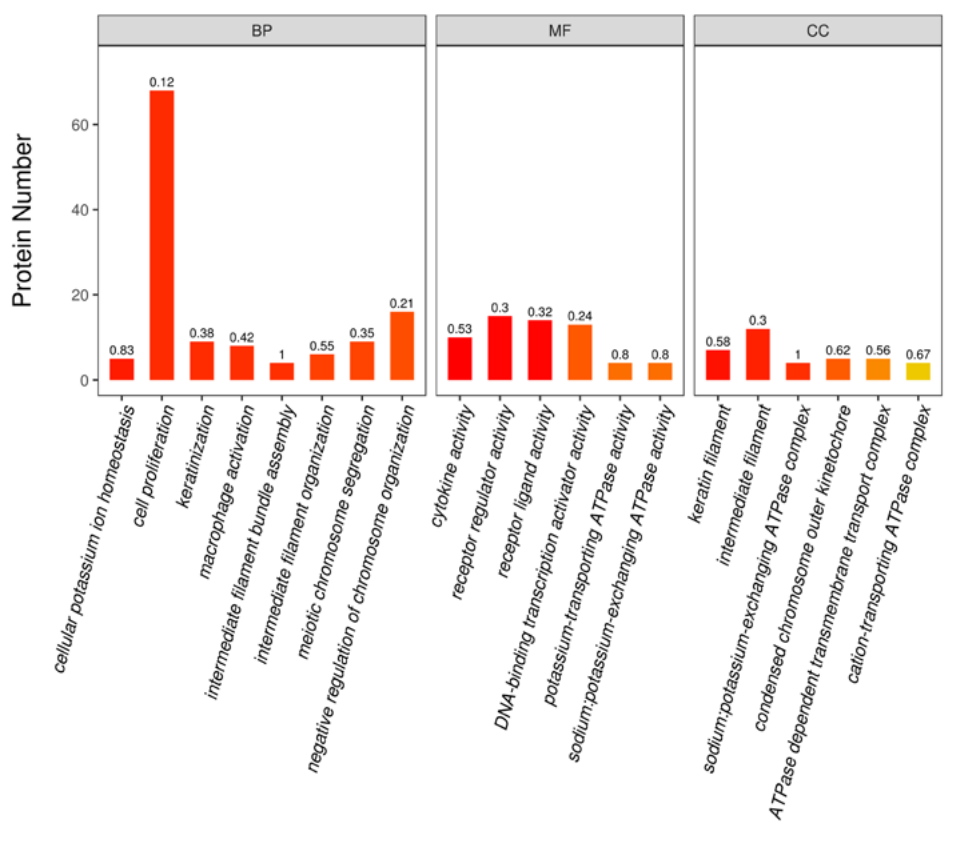


Fig. 6. The Gene Ontology (GO) functional enrichment analysis of the differentially expressed proteins. The x-axis represents the enriched GO functional classification, divided into biological process (BP), molecular function (MF) and cellular component (CC). The ordinate indicates the number of differentially expressed proteins. The color of the bar chart indicates the significance of the enriched GO functional classification. The label at the top of the bar chart shows the enrichment factor (richFactor ≤1), which refers to the ratio of the differentially expressed protein relative to all identified proteins

p.value

3e-04

2e-04



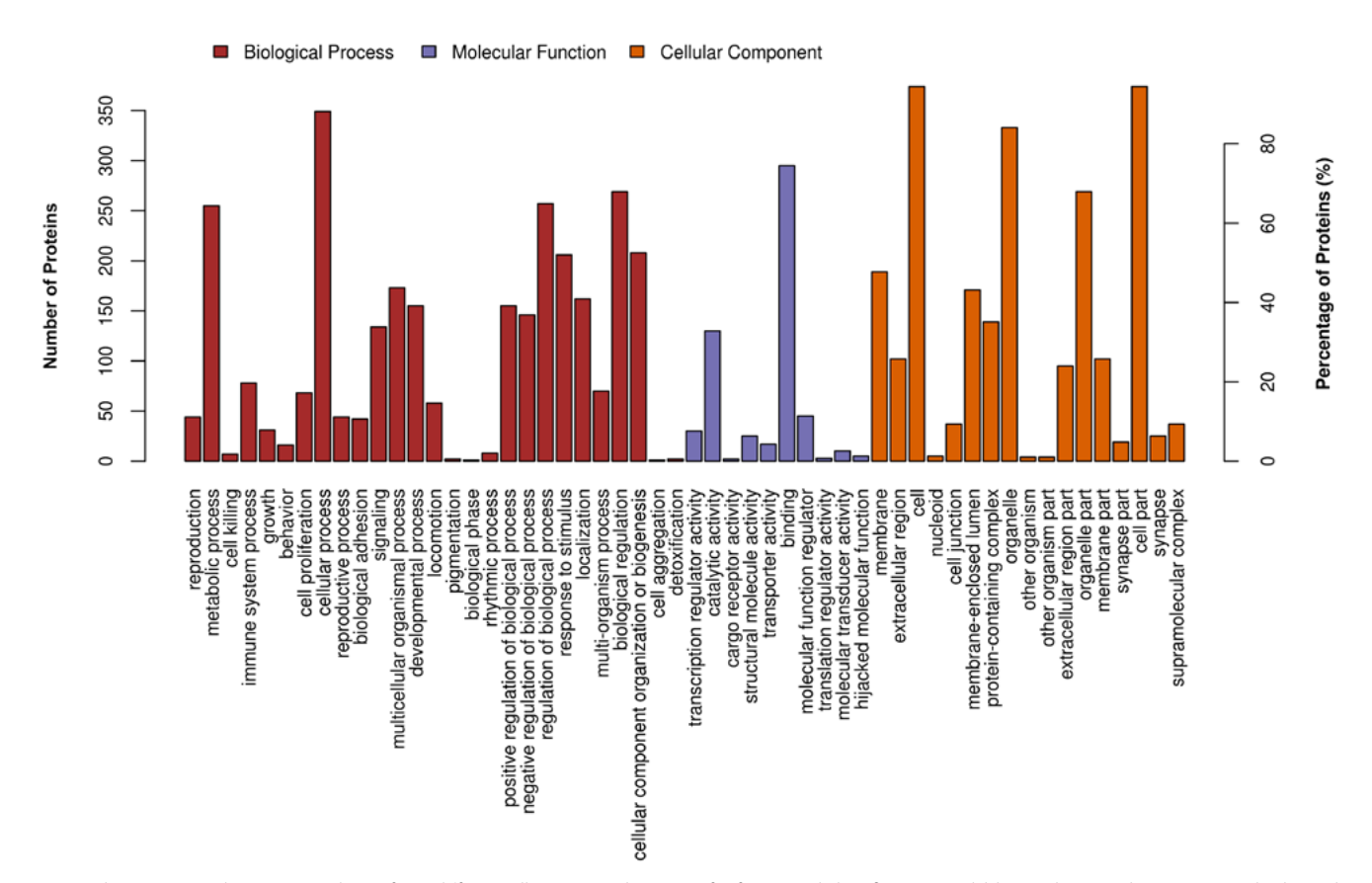


Fig. 7. The Gene Ontology (GO) analysis of 369 differentially expressed proteins for functional classification. Red, blue and orange bars represent biological processes, molecular functions and cellular components, respectively, ranking terms in the same category according to p-values. The ordinates on the left and right represent the number of differentially expressed proteins and their percentage within the differentially expressed proteins

# **KEGG** analysis

To identify the biological pathways related to differentially expressed proteins, KEGG was conducted. The proteins were found to be involved in 261 KEGG pathways. The top 20 significant pathways are: protein digestion and absorption, transcriptional misregulation in cancer, cardiac muscle contraction, bile secretion, malaria, proximal tubule bicarbonate reclamation, aldosterone-regulated sodium reabsorption, gastric acid secretion, mineral absorption, cytokine-cytokine receptor interaction, insulin secretion, Fanconi anemia pathway, carbohydrate digestion and absorption, viral myocarditis, p53 signaling pathway, *Staphylococcus aureus* infection, estrogen signaling pathway, PPAR signaling pathway, primary bile acid biosynthesis, and bladder cancer (Fig. 8).

# Differentially expressed proteins validated with PRM

In order to further confirm the iTRAQ results, we selected 6 differentially expressed proteins for quantitative PRM analysis. The PRM results (Table 4) exhibited the same trends as the data detected using iTRAQ, indicating that the originally obtained data are reliable.

### Discussion

The crude extract or the active components of CP, such as periplocin and PPG, have been investigated for hindering the growth of cancers, including pancreatic

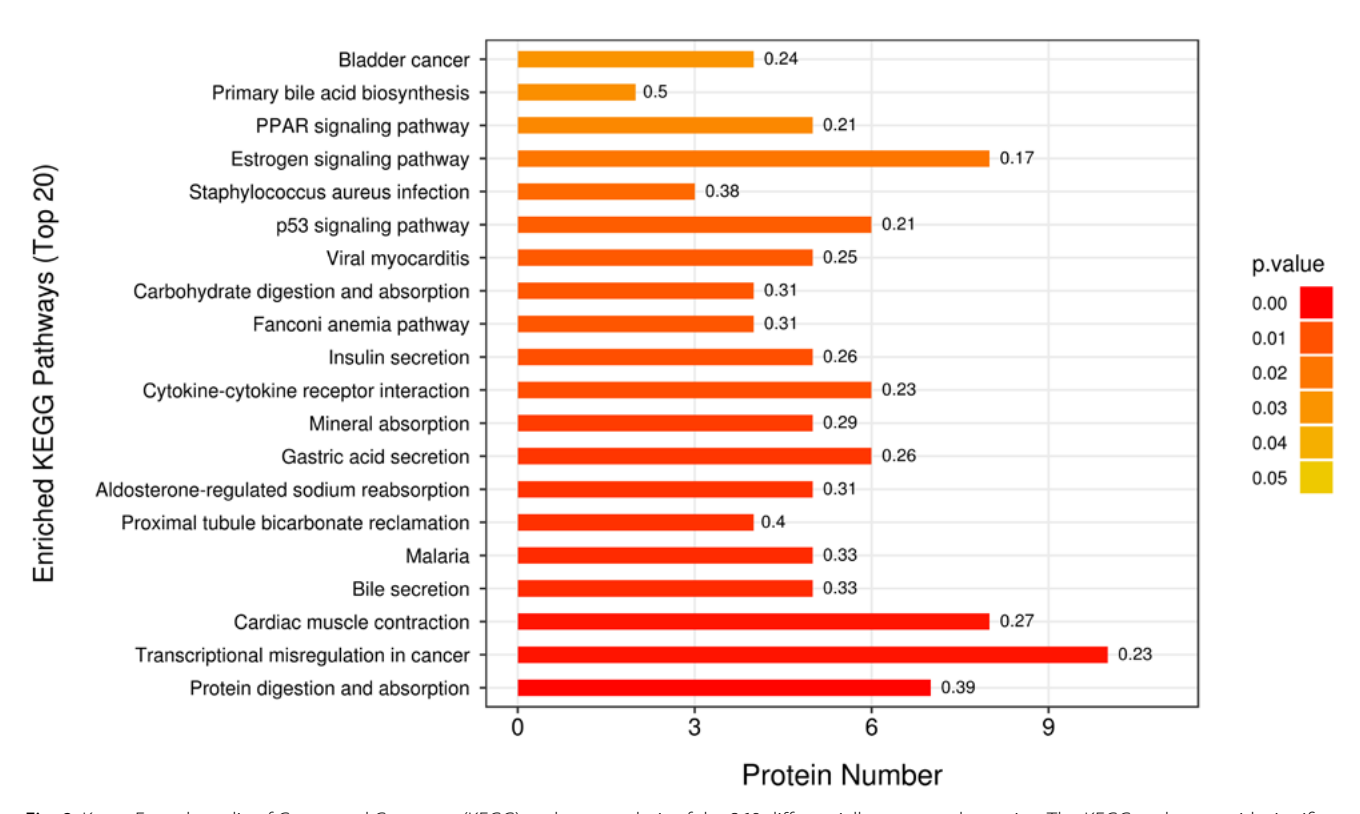


Fig. 8. Kyoto Encyclopedia of Genes and Genomes (KEGG) pathway analysis of the 369 differentially expressed proteins. The KEGG pathways with significant enrichment are represented by the ordinate. The horizontal axis shows the number of differentially expressed proteins included in each KEGG pathway. The color of the bar chart indicates the significance of the enriched KEGG pathway. The label at the top of the bar chart shows the enrichment factor (richFactor ≤1), which refers to the ratio of the differentially expressed proteins relative to all identified proteins

**Table 4.** Quantitative results for 14 candidate proteins determined using the parallel reaction monitoring (PRM)

Protein name	Average_C	Average_T	Ratio_T/C	TTEST_T/C
P08238	43.06311	30.39073	0.705725419	0.006075415
P11388	1.6252	2.30856	1.420479392	0.087019915
P05023	6.85455	12.97942	1.893549629	0.142457108
Q15582	1.28649	3.26519	2.538055779	0.137229876
P05026	3.307	5.24357	1.585595508	0.004255904
P04818	2.09784	0.99814	0.475794078	0.000295652

Student's t-test was used to calculate the p-values of groups T and C. Average\_C is the average of the 3 repetitive protein expression in group C. Average\_T is the average of the 3 repetitive protein expression in group T. Ratio\_T/C is the p-value of t-test.

cancer, gastric cancer, colon cancer, lung cancer, and nasopharyngeal cancer. In this study, the ethanol extract of CP inhibited the proliferation of U251 and TG905 cells, and induced cell cycle arrest and apoptosis. To find the specific active components responsible for the antitumor pharmacological properties, the network pharmacology analysis was conducted. We found 16 active components, namely poriferast-5-en-3beta-ol, beta-sitosterol, sitosterol, 21-O-Methyl-5,14-pregndiene-3 $\beta$ ,14 $\beta$ ,17 $\beta$ ,21-tetrol-20-one, 21-O-Methyl-5-pregnene-3 $\beta$ ,14 $\beta$ ,17 $\beta$ ,20,21-pentol, glycoside K\_qt, glycoside H2\_qt, glycozolidal, PPG, glycoside E\_qt, periplocoside M\_qt, delta 5-pregnenetriol, periplocoside O\_qt, periplocymarin\_qt, neridienone A, and xysmalogenin.

Several reports have illustrated that beta-sitosterol inhibits the proliferation of a range of cancer cell lines related to the activation of cell cycle arrest31,32 and stimulation of cellular apoptosis,33 which are consistent with our findings. Beta-sitosterol isolated from various plants accelerates apoptosis by stimulating the apoptosis pathway34 and the PI3K-AKT pathway.35 Wang et al. reported that beta-sitosterol reverses drug resistance in colorectal cancer via the p53 signaling pathway.<sup>36</sup> In our study, results from both integrated network pharmacology and iTRAQ-based quantitative proteomics technology demonstrated the activation of the p53 pathway, apoptosis pathway and PI3K-AKT signaling pathway in glioma cells after treatment with CP extract. Additionally, β-sitosterol plays an important role in treating prostate, lung, ovarian, colon, breast, and stomach cancer.37

Periplogenin was first isolated from the chloroform extract of CP in 1987, which clearly decreased the proliferation of ascite-associated cancer S<sub>180</sub> cells. <sup>38</sup> Li et al. reported that PPG strongly inhibited the proliferation of A2780, BGC823, PC3, Bel-7402, U937, A549, and HCT-8 cell lines in vitro with 0.66–3.16 uM IC50 values. <sup>39</sup> Currently, researchers have suggested that PPG may activate the ROS-ER stress pathway to stimulate apoptosis in colon cancer. <sup>17</sup> In nasopharyngeal cancer, PPG is related to the triggering of the PI3K-AKT signaling pathway. <sup>18</sup> The results reported by other researchers are consistent with our findings based on the network pharmacology and iTRAQ-based quantitative proteomics.

In addition to the abovementioned pathways, our findings showed that the Kaposi sarcoma-associated herpes virus infection pathway, the calcium signaling pathway, the transcriptional misregulation in cancer pathway, and others are involved in the CP-induced glioma treatment. The iTRAQ-based quantitative proteomics analysis also showed that there were 6 important differentially expressed proteins (HSP90AB1, TOP2A, ATP1A1, TGF $\beta$ 1, ATP1B1, and TYMS) found in CP-treated U251 cells compared with the control group. The specific functions of these proteins should be investigated further in future studies.

### Limitations

There are several limitations to this study. First, it is not clear which component of CP plays the anti-glioma role. Second, we only performed an in vitro cell study; further in vivo animal studies are needed to confirm this finding.

# **Conclusions**

In this study, we revealed that the extract of CP inhibited the proliferation of U251 and TG905 cells, and induced cell cycle arrest and apoptosis. We also found 16 active compounds of CP. Additionally, 6 proteins (HSP90AB1, TOP2A, ATP1A1, TGF $\beta$ 1, ATP1B1, and TYMS) were identified as the key factors involved in the regulation of CP in glioma. This study sheds light on the underlying molecular mechanisms mediated by CP effects in glioma.

#### **ORCID** iDs

Jing Huan https://orcid.org/0009-0003-1071-2458
Cui-Ping You https://orcid.org/0000-0002-3145-7236
Yu-Cheng Lu https://orcid.org/0000-0003-1510-9351
Feng-Yuan Che https://orcid.org/0000-0001-6551-2072

#### References

- Goodenberger ML, Jenkins RB. Genetics of adult glioma. Cancer Genet. 2012;205(12):613–621. doi:10.1016/j.cancergen.2012.10.009
- 2. Ostrom QT, Gittleman H, Liao P, et al. CBTRUS Statistical Report: Primary brain and central nervous system tumors diagnosed in the United States in 2007–2011. *Neurooncology*. 2014;16(Suppl 4): iv1–iv63. doi:10.1093/neuonc/nou223
- Ferlay J, Soerjomataram I, Dikshit R, et al. Cancer incidence and mortality worldwide: Sources, methods and major patterns in GLOBOCAN 2012. Int J Cancer. 2015;136(5):E359–E386. doi:10.1002/ijc.29210
- Hervey-Jumper SL, Berger MS. Maximizing safe resection of low- and high-grade glioma. J Neurooncol. 2016;130(2):269–282. doi:10.1007/ s11060-016-2110-4
- Krivosheya D, Prabhu SS, Weinberg JS, Sawaya R. Technical principles in glioma surgery and preoperative considerations. *J Neurooncol*. 2016;130(2):243–252. doi:10.1007/s11060-016-2171-4
- Wang J, Wang Y, He Y, et al. Radiotherapy versus radiotherapy combined with temozolomide in high-risk low-grade gliomas after surgery: Study protocol for a randomized controlled clinical trial. *Trials*. 2019; 20(1):641. doi:10.1186/s13063-019-3741-5
- Sørensen MD, Fosmark S, Hellwege S, Beier D, Kristensen BW, Beier CP. Chemoresistance and chemotherapy targeting stem-like cells in malignant glioma. Adv Exp Med Biol. 2015;853:111–138. doi:10.1007/ 978-3-319-16537-0 7
- Park SB, Goldstein D, Krishnan AV, et al. Chemotherapy-induced peripheral neurotoxicity: A critical analysis. CA Cancer J Clin. 2013; 63(6):419–437. doi:10.3322/caac.21204
- Li Y, Li J, Zhou K, et al. A review on phytochemistry and pharmacology of Cortex periplocae. Molecules. 2016;21(12):1702. doi:10.3390/molecules21121702
- Xie G, Sun L, Li Y, Chen B, Wang C. Periplocin inhibits the growth of pancreatic cancer by inducing apoptosis via AMPK-mTOR signaling. *Cancer Med.* 2021;10(1):325–336. doi:10.1002/cam4.3611
- He J, Bo F, Tu Y, et al. A validated LC–MS/MS assay for the simultaneous determination of periplocin and its two metabolites, periplocymarin and periplogenin in rat plasma: Application to a pharmacokinetic study. *J Pharm Biomed Anal*. 2015;114:292–295. doi:10.1016/j. jpba.2015.06.008
- 12. Tokiwa T, Harada K, Matsumura T, Tukiyama T. Oriental medicinal herb, *Periploca sepium*, extract inhibits growth and IL-6 production of human synovial fibroblast-like cells. *Biol Pharm Bull*. 2004;27(10): 1691–1693. doi:10.1248/bpb.27.1691

- Wan J, Zhu YN, Feng JQ, et al. Periplocoside A, a pregnane glycoside from Periploca sepium Bge, prevents concanavalin A-induced mice hepatitis through inhibiting NKT-derived inflammatory cytokine productions. *Int Immunopharmacol*. 2008;8(9):1248–1256. doi:10.1016/j. intimp.2008.05.001
- Li L, Zhao LM, Dai SL, et al. Periplocin extracted from cortex periplocae induced apoptosis of gastric cancer cells via the ERK1/2-EGR1 pathway. Cell Physiol Biochem. 2016;38(5):1939–1951. doi:10.1159/000445555
- Zhao L, Shan B, Du Y, Wang M, Liu L, Ren FZ. Periplocin from Cortex periplocae inhibits cell growth and downregulates survivin and c-myc expression in colon cancer in vitro and in vivo via β-catenin/TCF signaling. Oncol Rep. 2010;24(2):375–383. doi:10.3892/or\_00000870
- Lu ZJ, Zhou Y, Song Q, et al. Periplocin inhibits growth of lung cancer in vitro and in vivo by blocking AKT/ERK signaling pathways. Cell Physiol Biochem. 2010;26(4–5):609–618. doi:10.1159/000322328
- Yang Y, Liu Y, Zhang Y, Ji W, Wang L, Lee SC. Periplogenin activates ROS-ER stress pathway to trigger apoptosis via BIP-eIF2α-CHOP and IRE1α-ASK1-JNK signaling routes. *Anticancer Agents Med Chem.* 2020; 21(1):61–70. doi:10.2174/1871520620666200708104559
- Ye H, Wei X, Meng C, et al. Mechanism of action of periplogenin on nasopharyngeal carcinoma based on network pharmacology and experimental study of vitamin E coupled with periplogenin self-assembled nano-prodrug for nasopharyngeal carcinoma. *J Biomed Nanotechnol*. 2020;16(9):1406–1415. doi:10.1166/jbn.2020.2978
- Wang L, Lu A, Meng F, Cao Q, Shan B. Inhibitory effects of lupeal acetate of *Cortex periplocae* on N-nitrosomethylbenzylamineinduced rat esophageal tumorigenesis. *Oncol Lett*. 2012;4(2):231–236. doi:10.3892/ol.2012.717
- Liu CM, Chen J, Yang S, et al. iTRAQ-based proteomic analysis to identify the molecular mechanism of Zhibai Dihuang Granule in the Yindeficiency-heat syndrome rats. *Chin Med*. 2018;13(1):2. doi:10.1186/s13020-017-0160-y
- 21. Wen JX, Li RS, Wang J, et al. Therapeutic effects of Aconiti Lateralis Radix Praeparata combined with *Zingiberis rhizoma* on doxorubicin-induced chronic heart failure in rats based on an integrated approach. *J Pharm Pharmacol*. 2020;72(2):279–293. doi:10.1111/jphp.13191
- Guo Q, Zheng K, Fan D, et al. Wu-Tou decoction in rheumatoid arthritis: Integrating network pharmacology and in vivo pharmacological evaluation. *Front Pharmacol*. 2017;8:230. doi:10.3389/fphar. 2017.00230
- 23. Wang X, Shen Y, Wang S, et al. PharmMapper 2017 update: A web server for potential drug target identification with a comprehensive target pharmacophore database. *Nucleic Acids Res.* 2017;45(W1): W356–W360. doi:10.1093/nar/gkx374
- The UniProt Consortium. UniProt: A worldwide hub of protein knowledge. Nucleic Acids Res. 2019;47(D1):D506–D515. doi:10.1093/nar/gky1049
- Huang J, Cheung F, Tan HY, et al. Identification of the active compounds and significant pathways of yinchenhao decoction based on network pharmacology. *Mol Med Rep.* 2017;16(4):4583–4592. doi:10.3892 /mmr.2017.7149

- 26. Huang C, Zheng C, Li Y, Wang Y, Lu A, Yang L. Systems pharmacology in drug discovery and therapeutic insight for herbal medicines. *Brief Bioinform*. 2014;15(5):710–733. doi:10.1093/bib/bbt035
- Warde-Farley D, Donaldson SL, Comes O, et al. The GeneMANIA prediction server: Biological network integration for gene prioritization and predicting gene function. *Nucleic Acids Res.* 2010;38(Suppl 2): W214–W220. doi:10.1093/nar/gkq537
- Wang J, Duncan D, Shi Z, Zhang B. WEB-based GEne SeT Analysis Toolkit (WebGestalt): Update 2013. Nucleic Acids Res. 2013;41(W1):W77–W83. doi:10.1093/nar/gkt439
- Wiśniewski JR, Zougman A, Nagaraj N, Mann M. Universal sample preparation method for proteome analysis. *Nat Methods*. 2009; 6(5):359–362. doi:10.1038/nmeth.1322
- Ross PL, Huang YN, Marchese JN, et al. Multiplexed protein quantitation in Saccharomyces cerevisiae using amine-reactive isobaric tagging reagents. Mol Cell Proteomics. 2004;3(12):1154–1169. doi:10.1074/mcp.M400129-MCP200
- Awad AB, von Holtz RL, Cone JP, Fink CS, Chen YC. Beta-sitosterol inhibits growth of HT-29 human colon cancer cells by activating the sphingomyelin cycle. *Anticancer Res.* 1998;18(1A):471–473. PMID:9568122.
- 32. Awad AB, Williams H, Fink CS. Phytosterols reduce in vitro metastatic ability of MDA-MB-231 human breast cancer cells. *Nutr Cancer*. 2001;40(2):157–164. doi:10.1207/S15327914NC402\_12
- Rajavel T, Packiyaraj P, Suryanarayanan V, Singh SK, Ruckmani K, Pandima Devi K. β-sitosterol targets Trx/Trx1 reductase to induce apoptosis in A549 cells via ROS mediated mitochondrial dysregulation and p53 activation. Sci Rep. 2018;8(1):2071. doi:10.1038/s41598-018-20311-6
- 34. Awad AB, Chinnam M, Fink CS, Bradford PG. β-sitosterol activates Fas signaling in human breast cancer cells. *Phytomedicine*. 2007;14(11): 747–754. doi:10.1016/j.phymed.2007.01.003
- Xu H, Li Y, Han B, et al. Anti-breast-cancer activity exerted by β-sitosterol-D-glucoside from sweet potato via upregulation of microRNA-10a and via the PI3K–Akt signaling pathway. *J Agric Food Chem.* 2018; 66(37):9704–9718. doi:10.1021/acs.jafc.8b03305
- 36. Wang Z, Zhan Y, Xu J, et al. β-sitosterol reverses multidrug resistance via BCRP suppression by inhibiting the p53–MDM2 interaction in colorectal cancer. *J Agric Food Chem.* 2020;68(12):3850–3858. doi:10.1021/acs.jafc.0c00107
- 37. Bin Sayeed MS, Ameen SS. Beta-sitosterol: A promising but orphan nutraceutical to fight against cancer. *Nutr Cancer*. 2015;67(8):1216–1222. doi:10.1080/01635581.2015.1087042
- Itokawa H, Xu J, Takeya K. Studies on chemical constituents of antitumor fraction from *Periploca sepium* BGE. I. Chem Pharm Bull. 1987; 35(11):4524–4529. doi:10.1248/cpb.35.4524
- Li Y, Liu YB, Yu SS, et al. Cytotoxic cardenolides from the stems of *Periploca forrestii*. Steroids. 2012;77(5):375–381. doi:10.1016/j.steroids.2011.12.013